1 Preindustrial climate variability

In Figs. S1 and S2, we show maps of the standard deviation over the preindustrial era for temperature and precipitation ETCCDI indices, respectively. In regions with low climate variability during this time period, emergence can occur even with a relatively small change in climate. In regions with high climate variability, only relatively large changes are likely to result in emergence being detected.

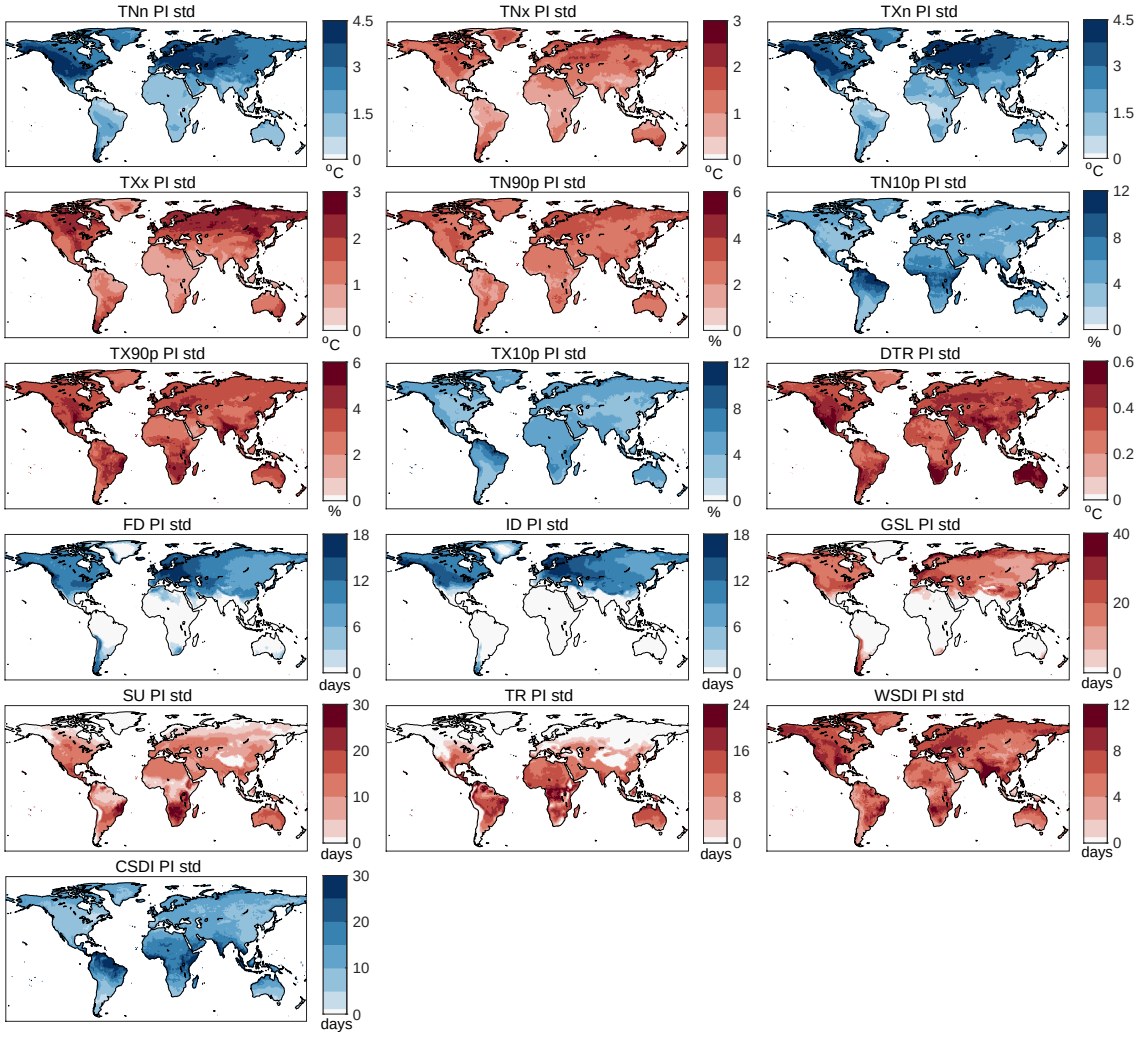

Figure S1. Standard deviation of annual temperature ETCCDI indices in the preindustrial period 1850–1900 as weighted median over one ensemble member of each CMIP6 model.

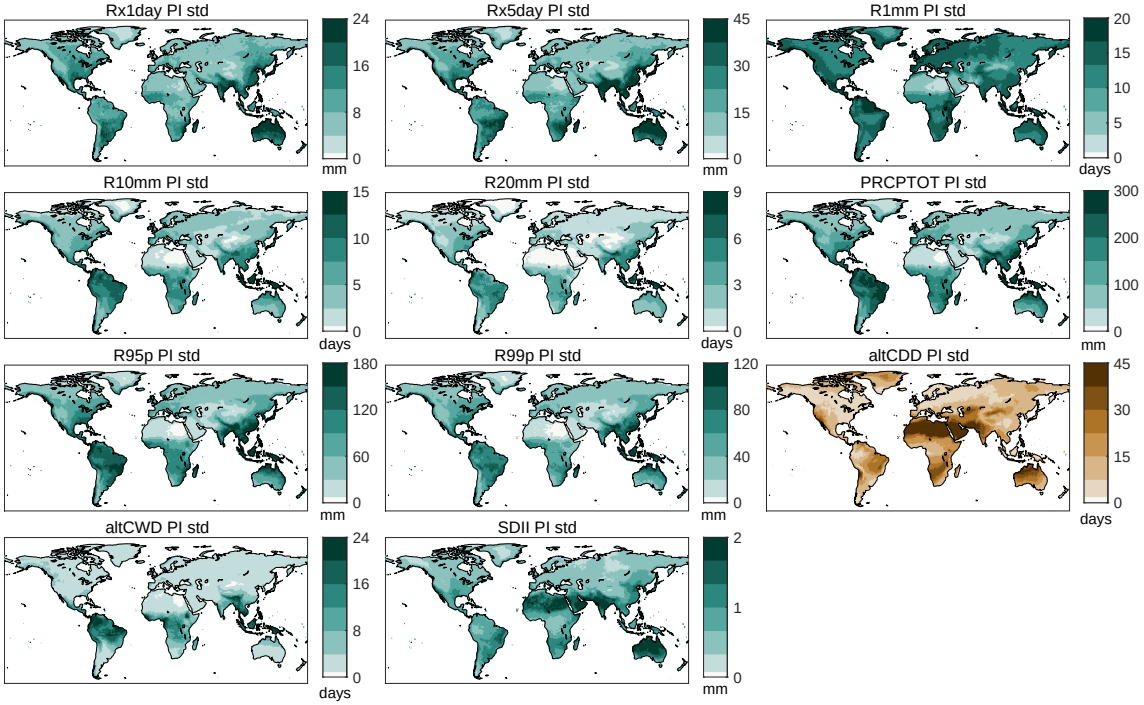

Figure S2. Standard deviation of annual precipitation ETCCDI indices in the preindustrial period 1850–1900 as weighted median over one ensemble member of each CMIP6 model.

2 Additional temperature indices

In Figs. S3–S13, we show results for the annual temperature-related ETCCDI indices not covered in the main article. In Figs. S14–S16, we show results for the seasonal "coldest night" (TNn) index and the seasons not covered in the main article.

2.1 Annual indices

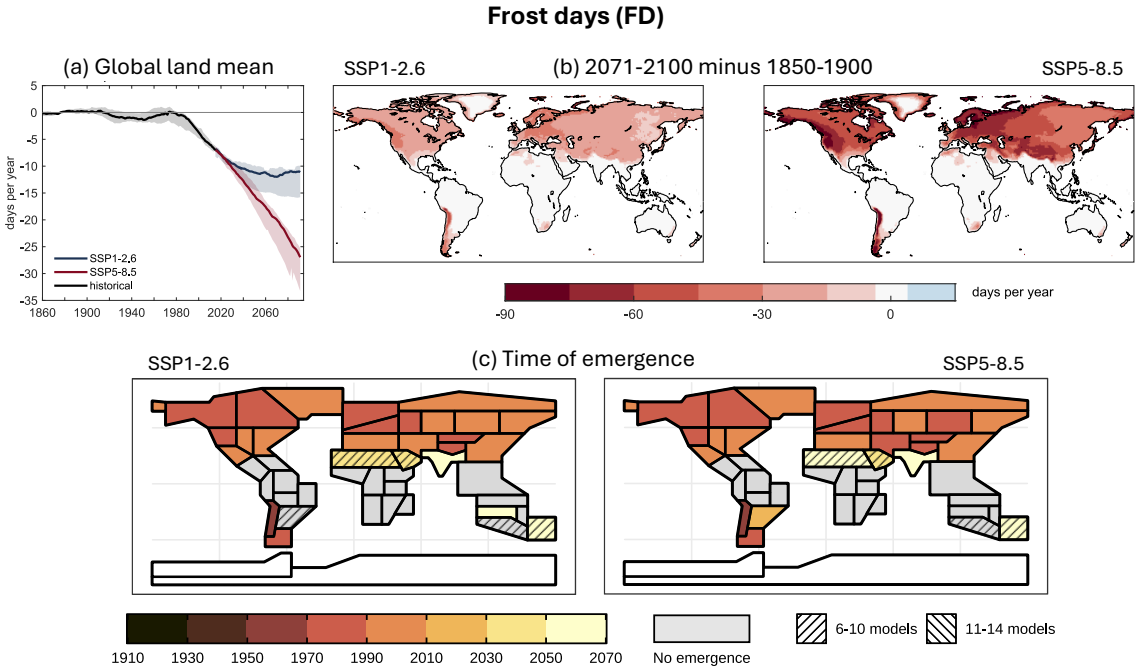

Figure S3. Frost days (FD): (a) Time series of global land mean FD (excluding Antarctica), as weighted median of all models, each contributing one ensemble member, with corresponding inter-quartile range, for the historical period (1850–2014) and emissions scenarios SSP1-2.6 and SSP5-8.5 (2015–2100), expressed as anomalies relative to the preindustrial period (1850–1900). (b) Difference between end of the 21st century (2071–2100) and preindustrial period (1850–1900) of the weighted multi-model median FD for SSP1-2.6 and SSP5-8.5, calculated from the same set of simulations. The colorbar is truncated at both end values. (c) FD time of emergence for IPCC AR6 reference regions and SSP1-2.6/SSP5-8.5 (weighted median of all available models and members), referring to the first year of any 20-year time period. Hatched regions indicate low agreement between models as to whether emergence occurs before 2070, with either 6–10 models (roughly 25–50%) or 11–14 (roughly 50–75%) out of 20 showing emergence.

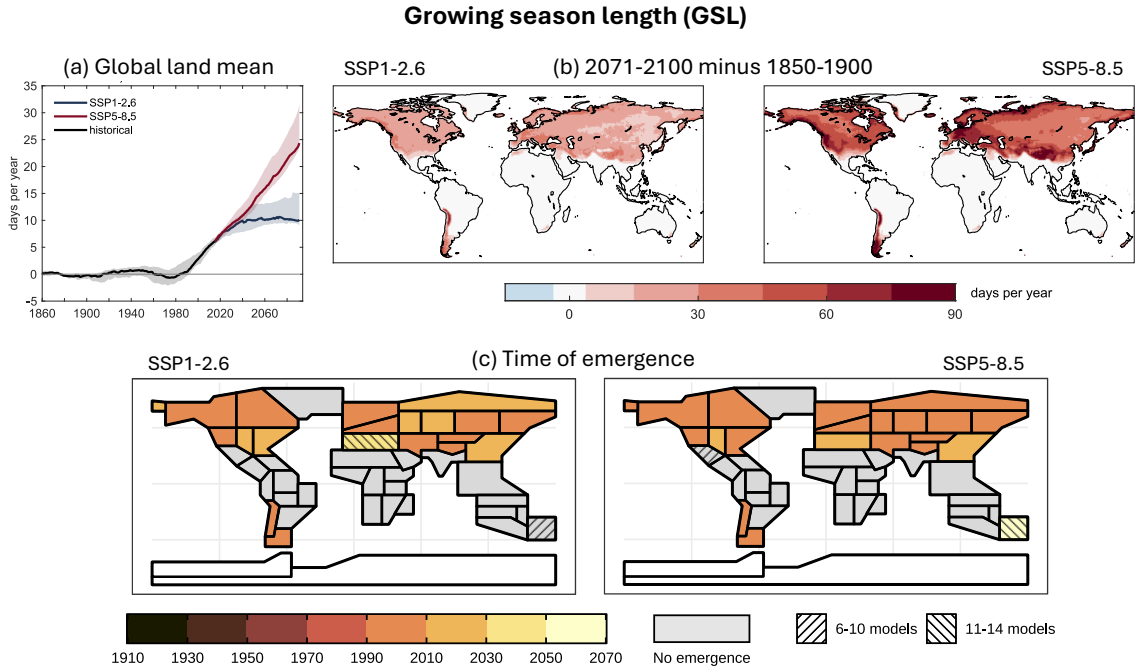

Figure S4. Same as Fig. S3, but for growing season length (GSL).

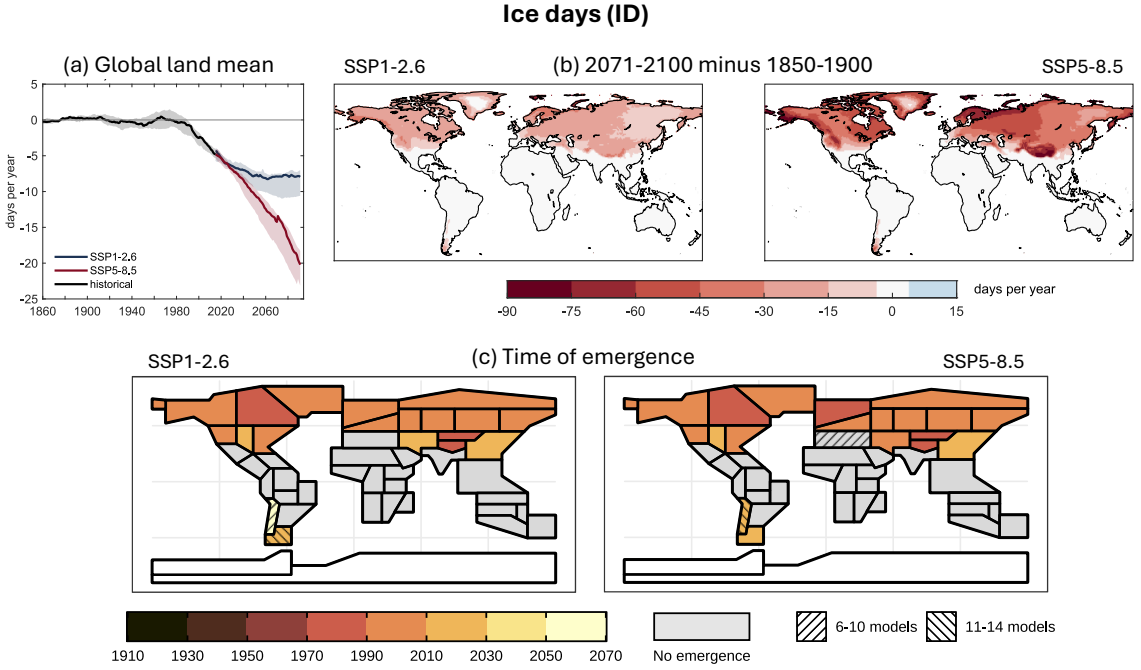

Figure S5. Same as Fig. S3, but for ice days (ID).

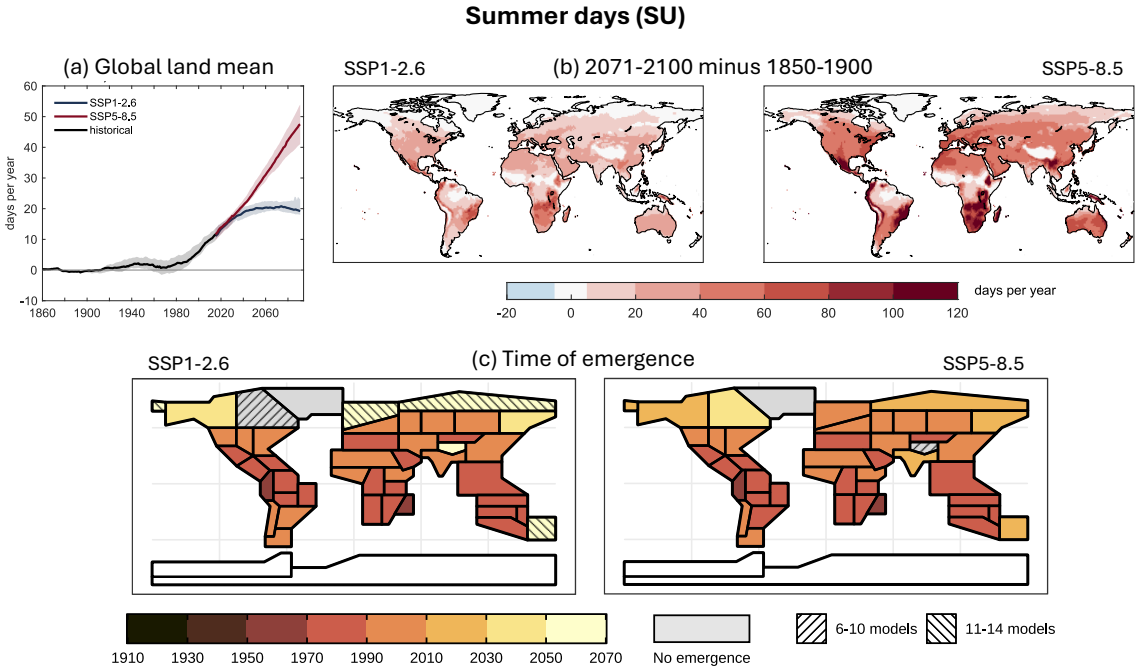

Figure S6. Same as Fig. S3, but for summer days (SU).

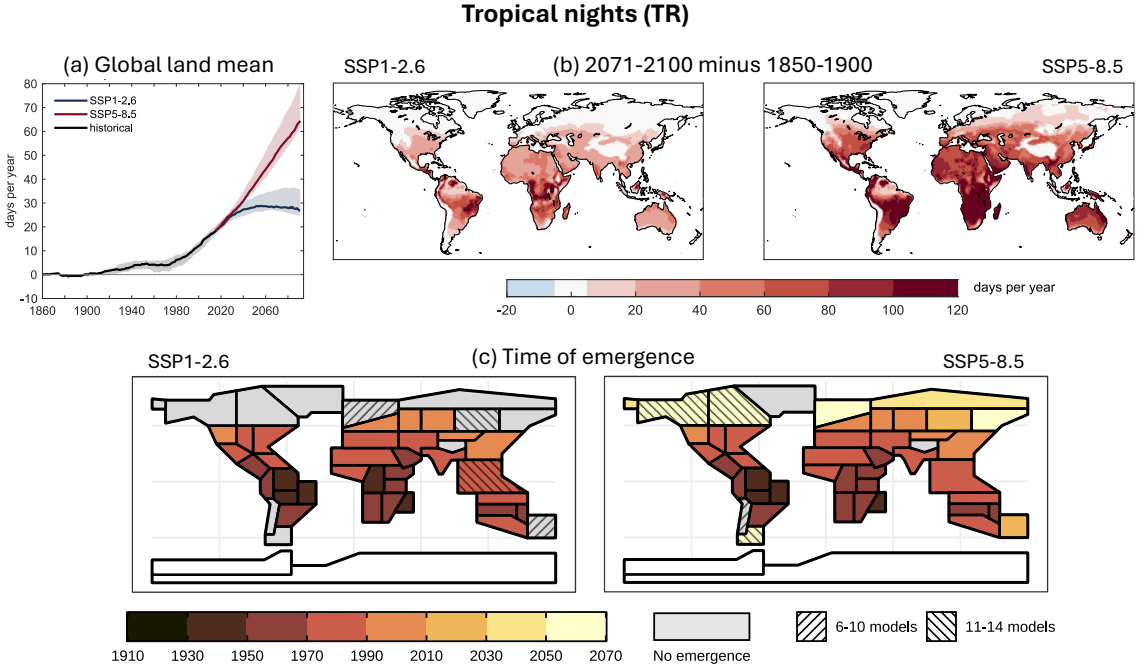

Figure S7. Same as Fig. S3, but for tropical nights (TR).

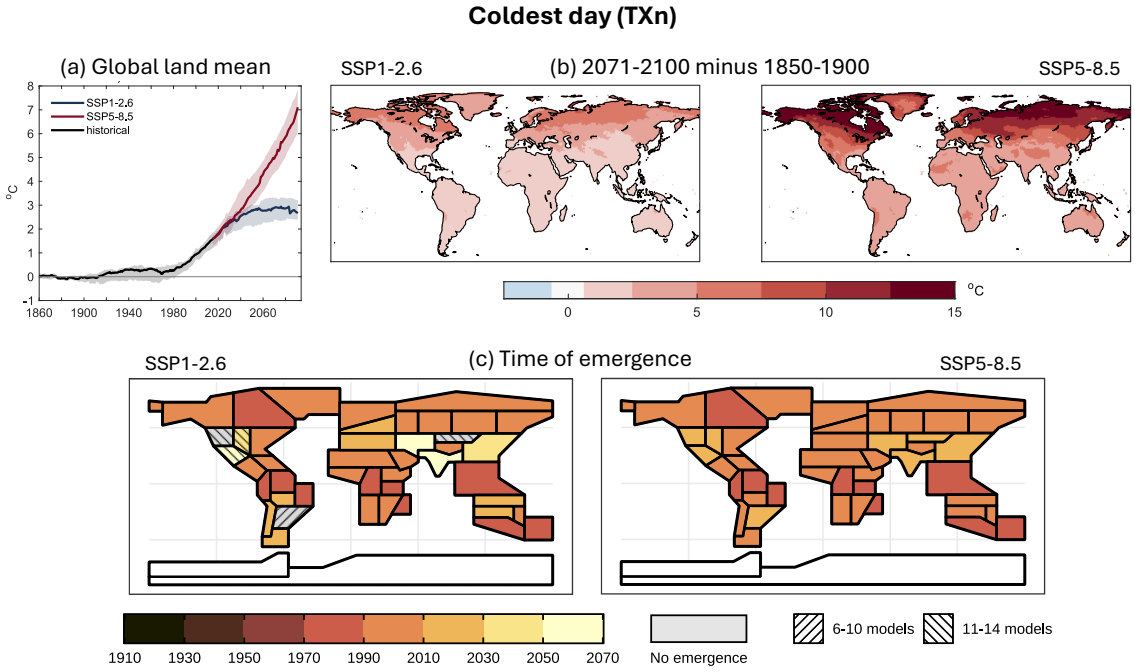

Figure S8. Same as Fig. S3, but for coldest day (TXn).

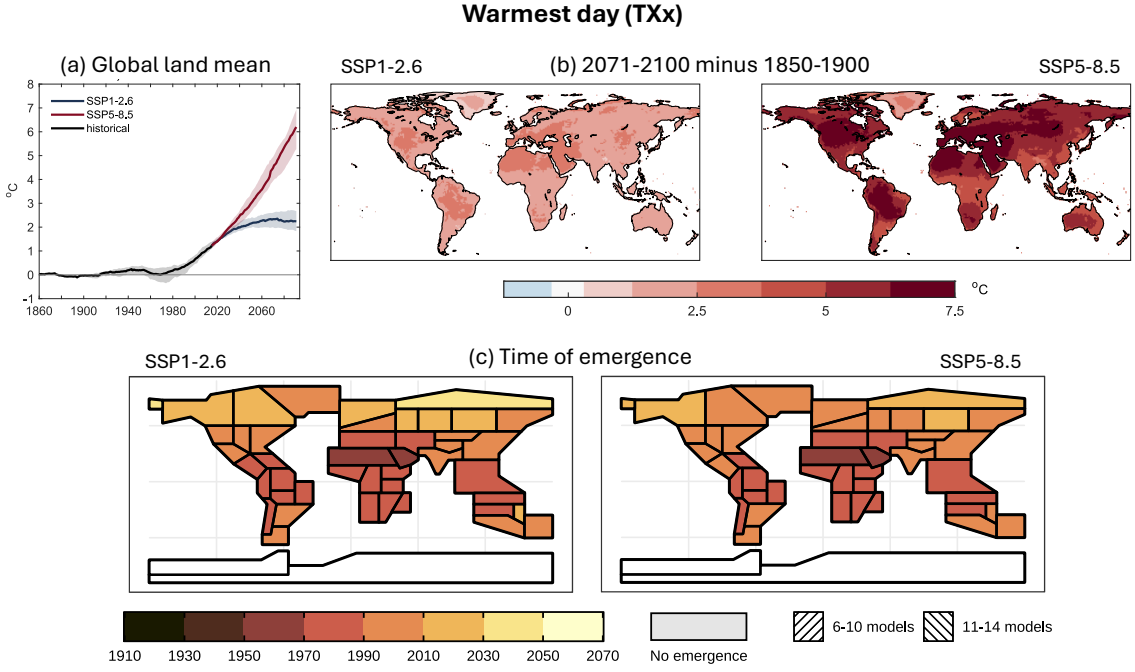

Figure S9. Same as Fig. S3, but for warmest day (TXx).

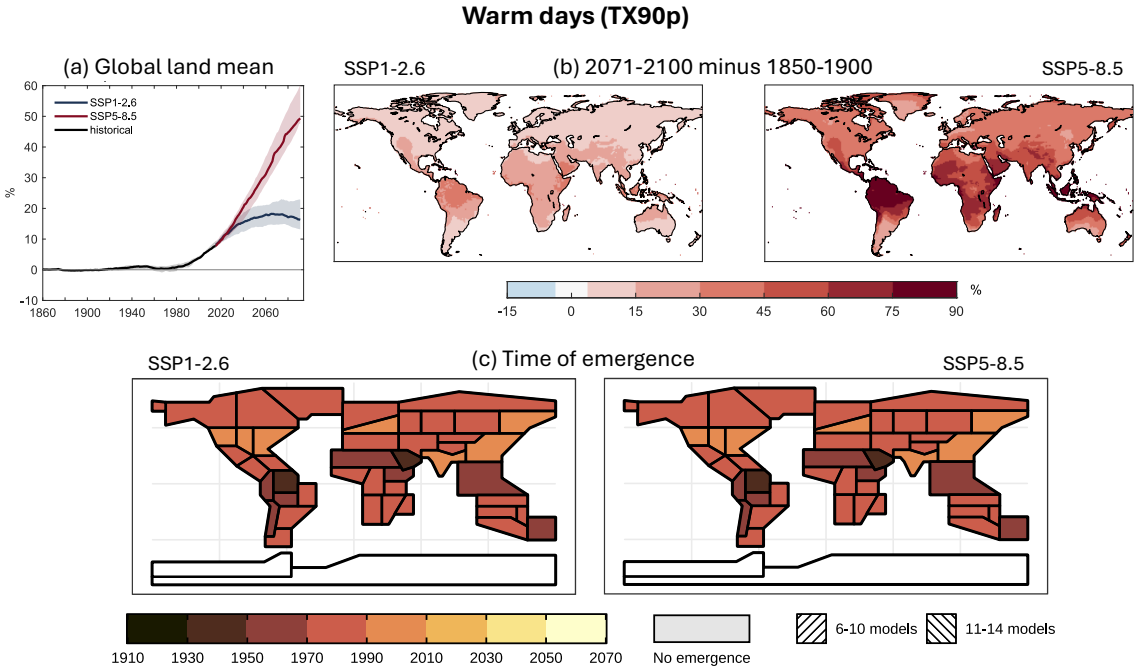

Figure S10. Same as Fig. S3, but for warm days (TX90p).

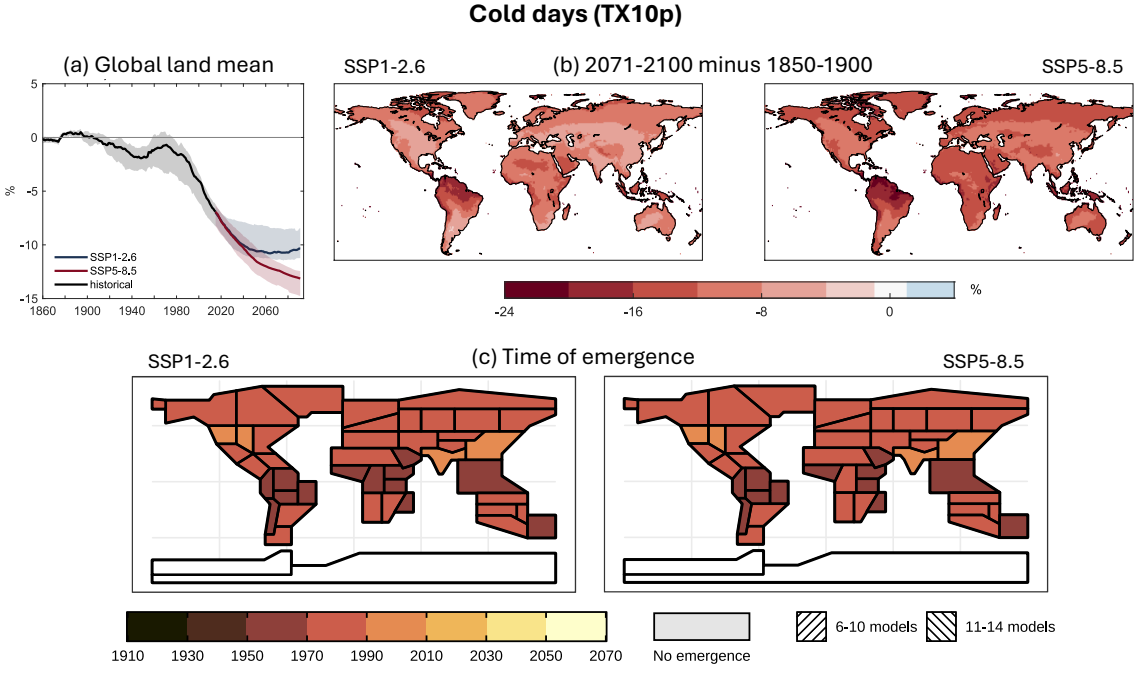

Figure S11. Same as Fig. S3, but for cold days (TX10p).

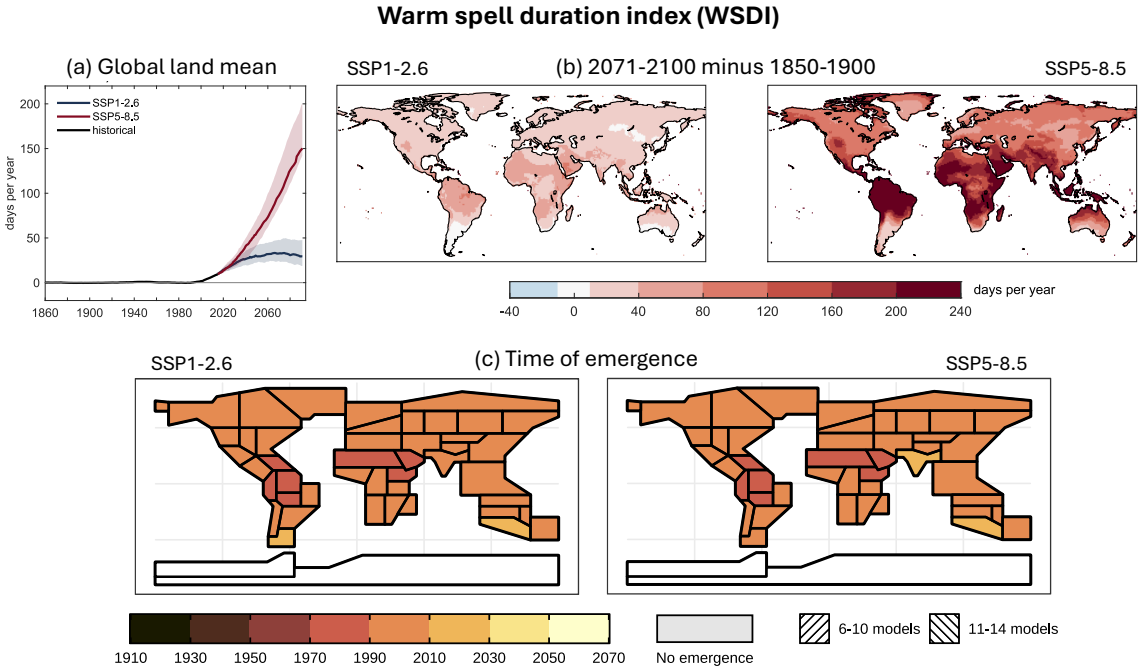

Figure S12. Same as Fig. S3, but for warm spell duration index (WSDI).

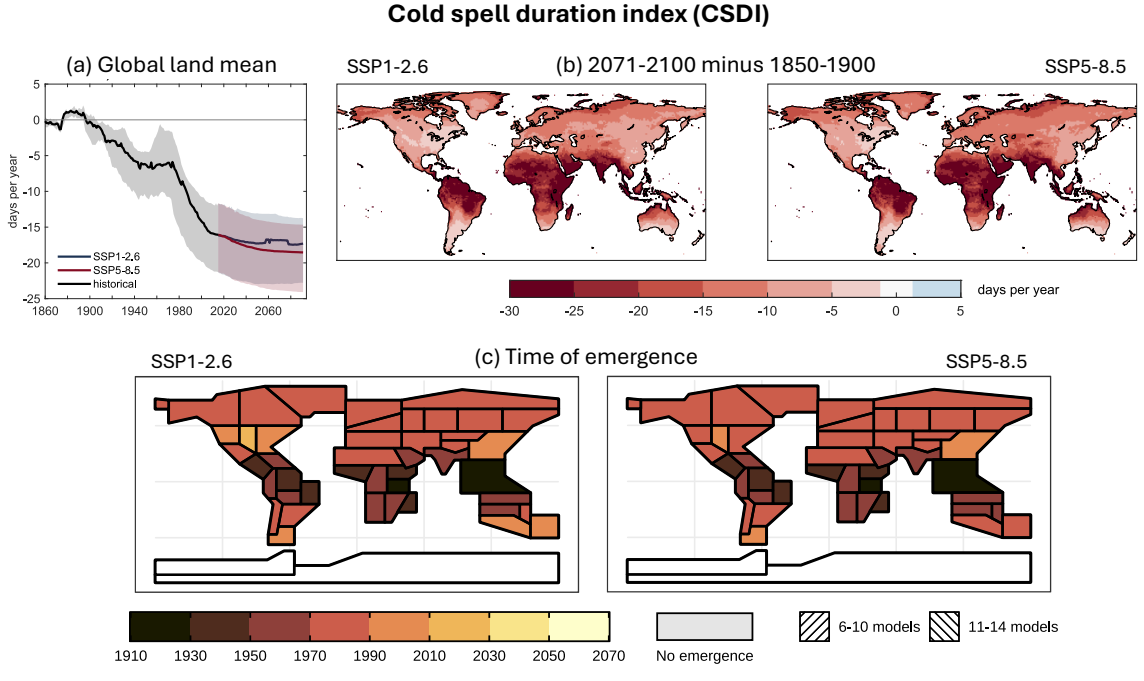

Figure S13. Same as Fig. S3, but for cold spell duration index (CSDI).

2.2 Seasonal indices

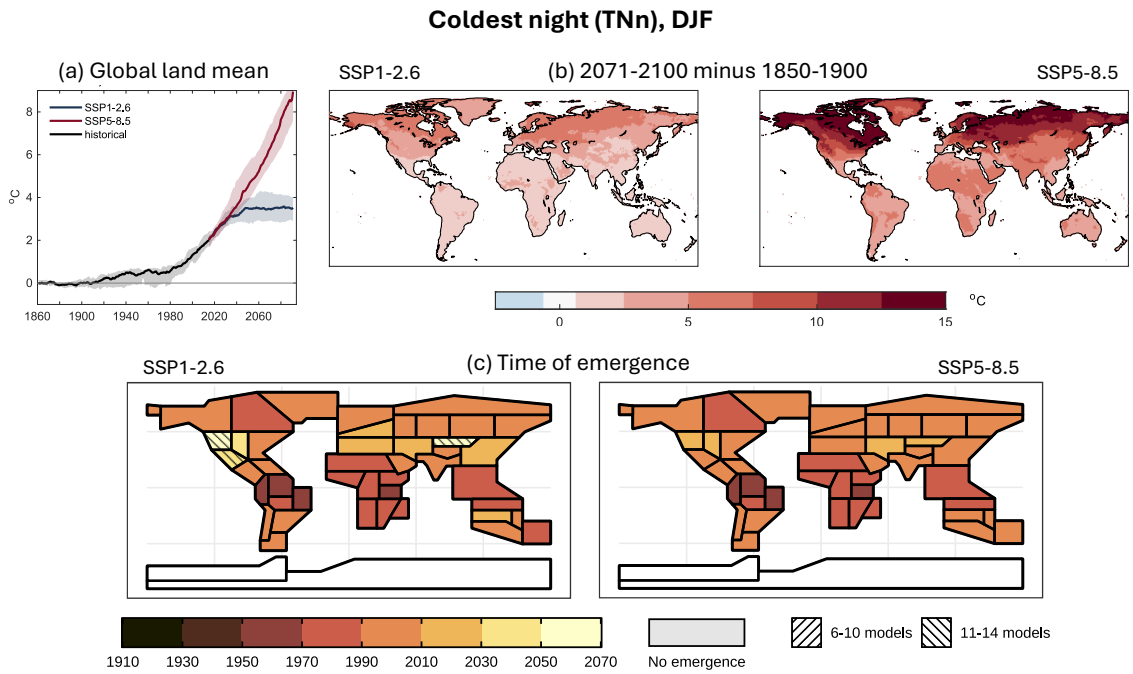

Figure S14. Same as Fig. S3, but for coldest night (TNn) during December/January/February.

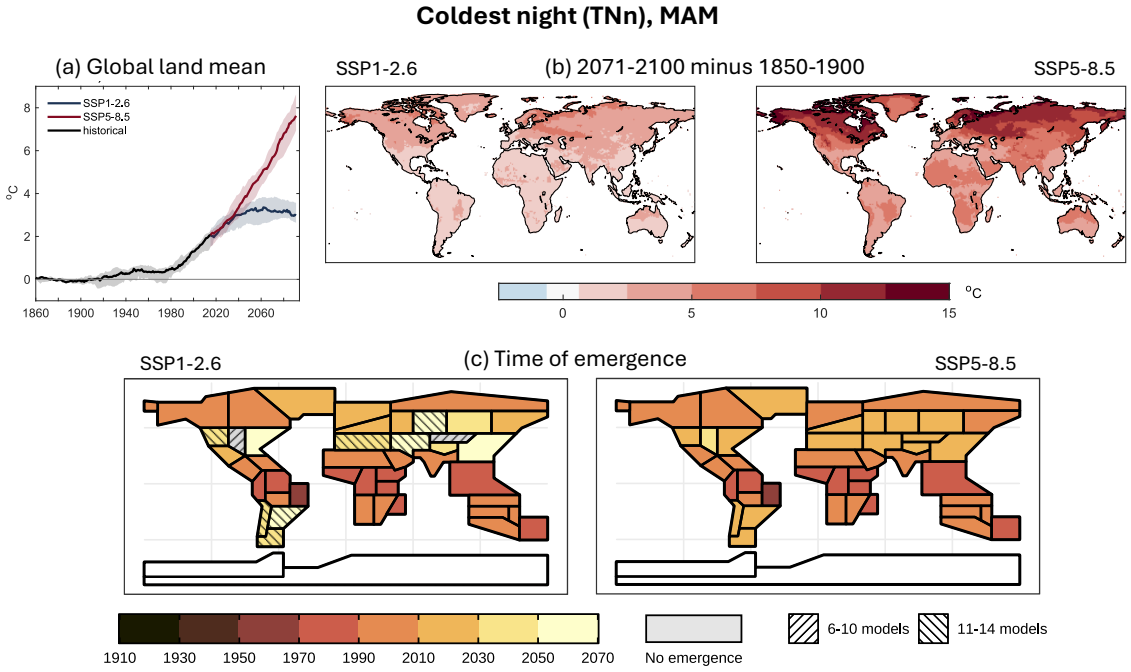

Figure S15. Same as Fig. S3, but for coldest night (TNn) during March/April/May.

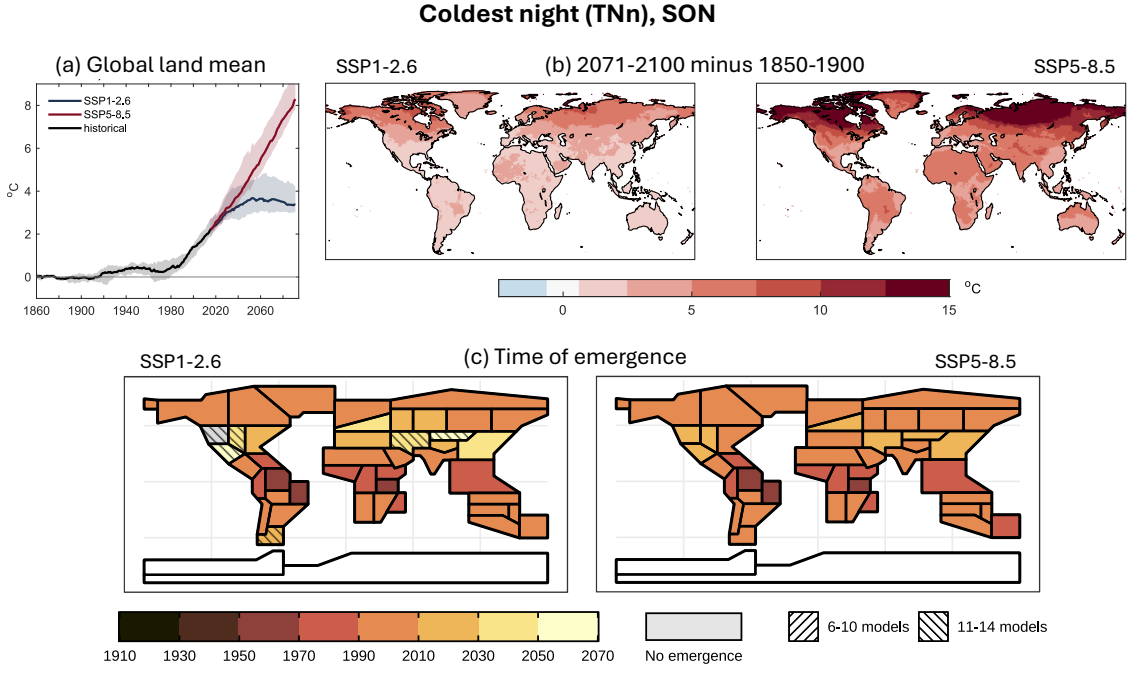

Figure S16. Same as Fig. S3, but for coldest night (TNn) during September/October/November.

3 Additional precipitation indices

3.1 Annual indices

In Figs. S17–S24, we show results for the annual precipitation-related ETCCDI indices not covered in the main article. In Figs. S25–S27, we show results for the seasonal "max 1-day precipitation" (Rx1day) index for those seasons not covered in the main article.

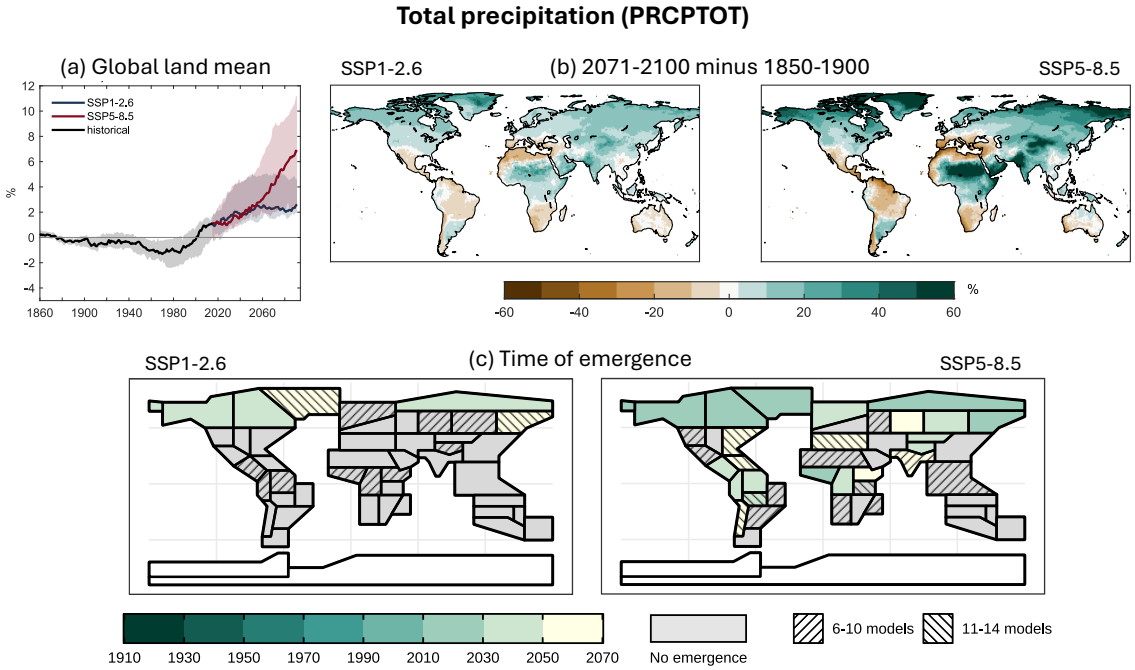

Figure S17. Total precipitation (PRCPTOT): (a) Time series of global land mean PRCPTOT (excluding Antarctica), as weighted median of all models, each contributing one ensemble member, with corresponding inter-quartile range, for the historical period (1850–2014) and emissions scenarios SSP1-2.6 and SSP5-8.5 (2015–2100), expressed as percentage anomalies relative to the preindustrial period (1850–1900). (b) Difference between end of the 21st century (2071–2100) and preindustrial period (1850–1900) of the weighted multi-model median PRCPTOT for SSP1-2.6 and SSP5-8.5, calculated from the same set of simulations. The colorbar is truncated at both end values. (c) Rx1day time of emergence for IPCC AR6 reference regions and SSP1-2.6/SSP5-8.5 (weighted median of all available models and members), referring to the first year of any 20-year time period. Hatched regions indicate low agreement between models as to whether emergence occurs before 2070, with either 6–10 models (roughly 25–50%) or 11–14 (roughly 50–75%) out of 21 showing emergence.

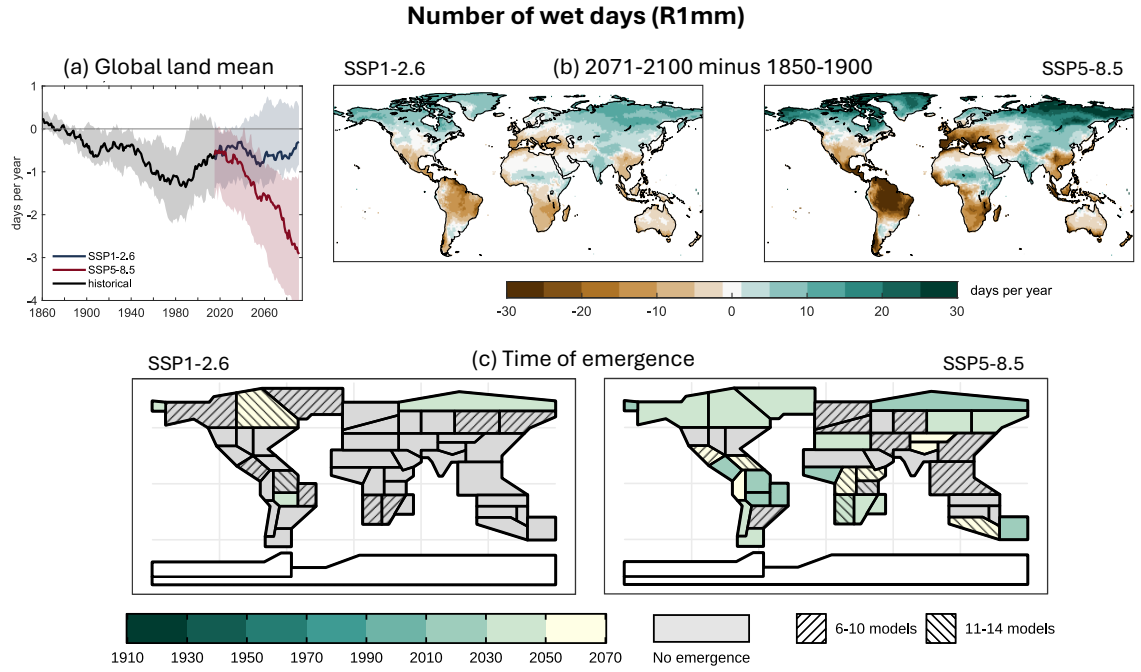

Figure S18. Same as Fig. S17, but for number of wet days (R1mm).

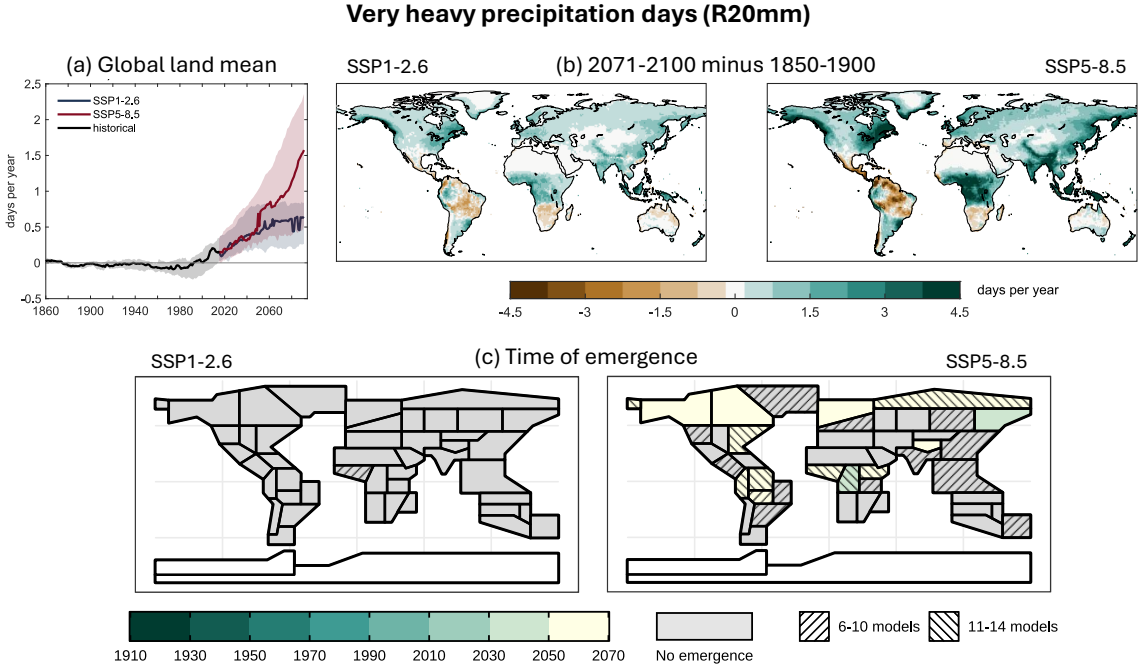

Figure S19. Same as Fig. S17, but for very heavy precipitation days (R20mm).

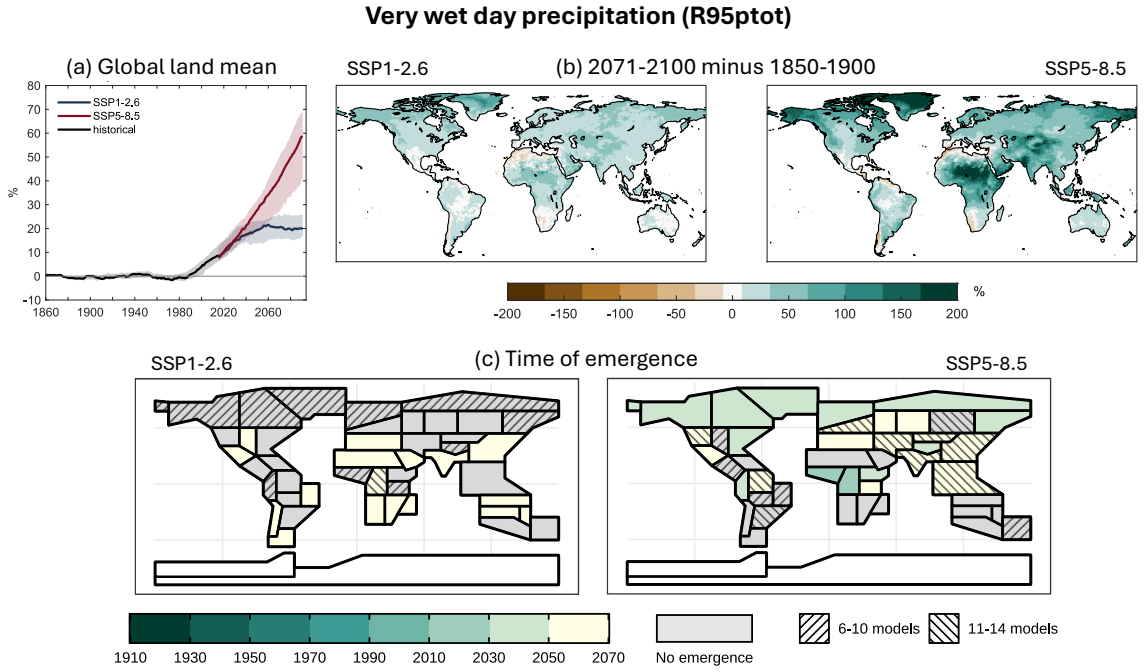

Figure S20. Same as Fig. S17, but for very wet day precipitation (R95ptot).

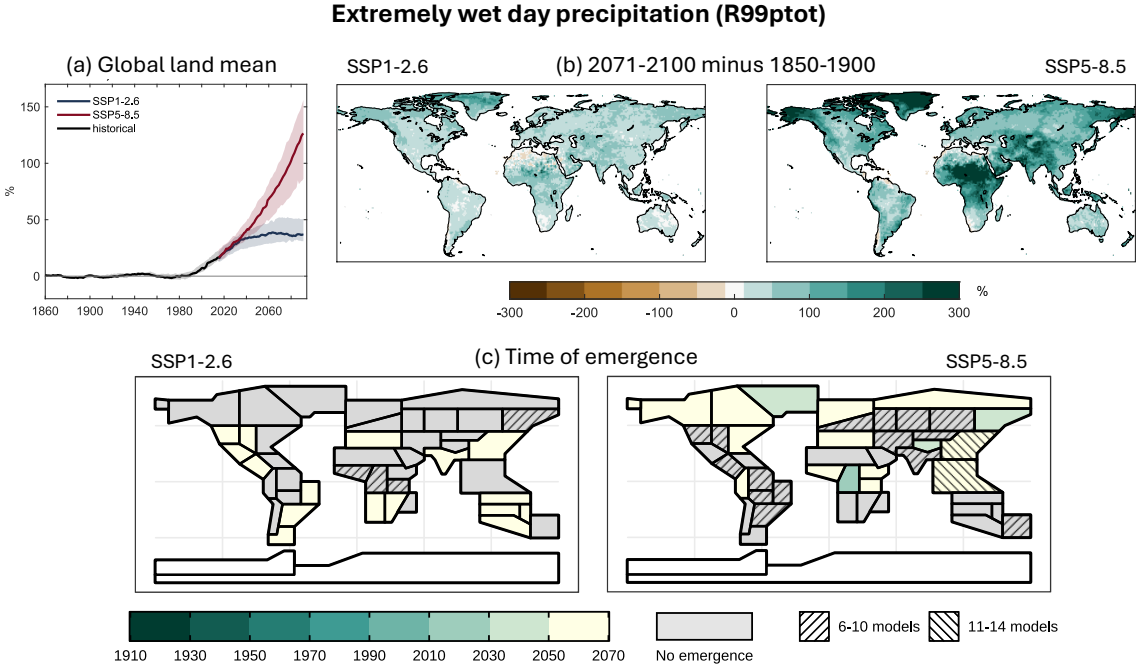

Figure S21. Same as Fig. S17, but for extremely wet day precipitation (R99ptot).

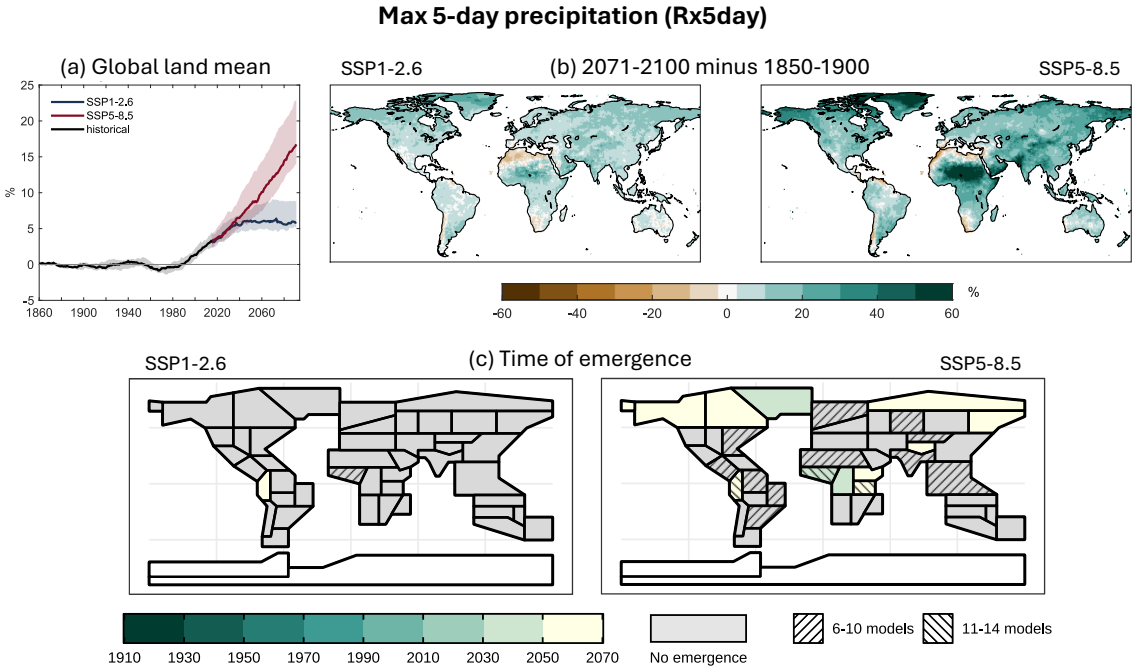

Figure S22. Same as Fig. S17, but for max 5-day precipitation (Rx5day).

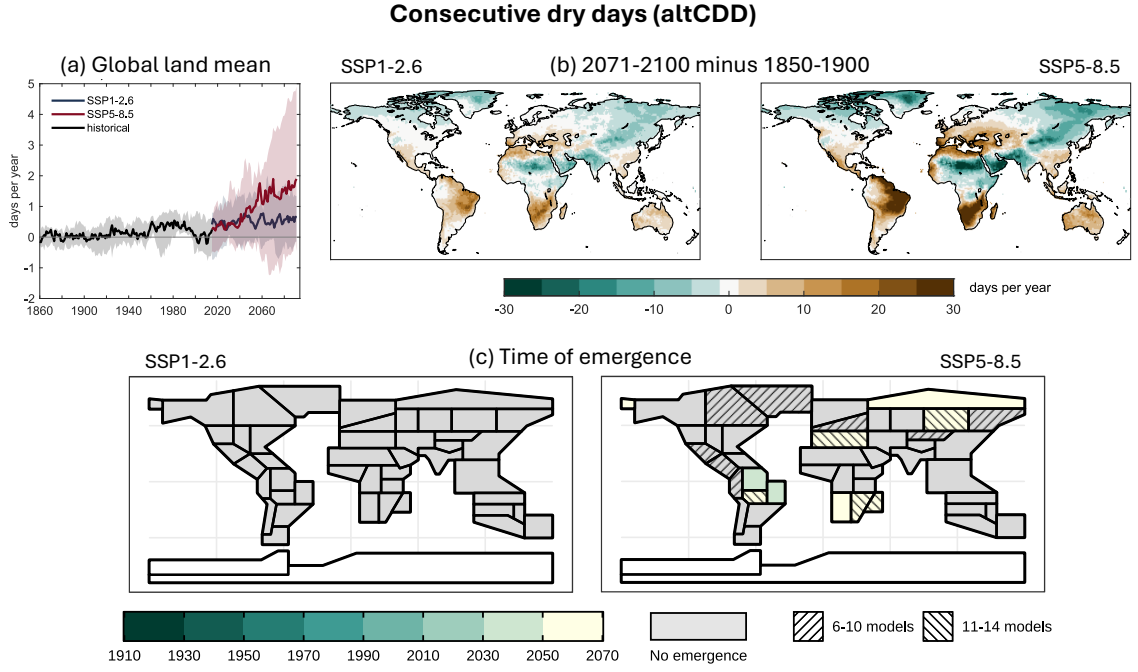

Figure S23. Same as Fig. S17, but for consecutive dry days (altCDD).

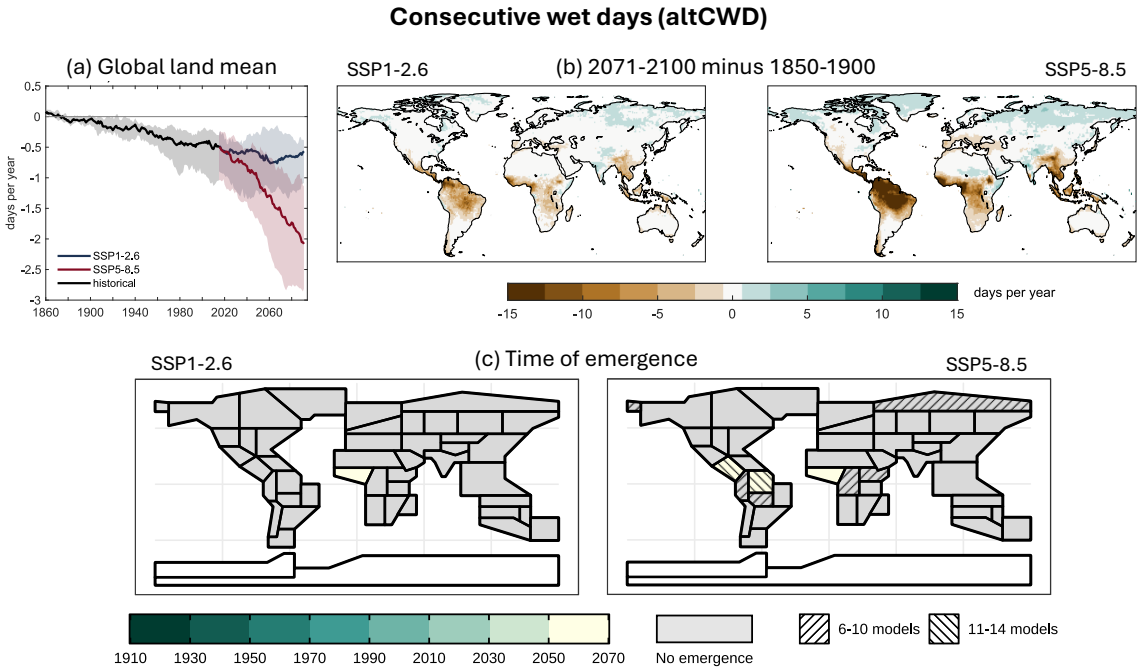

Figure S24. Same as Fig. S17, but for consecutive wet days (altCWD).

3.2 Seasonal indices

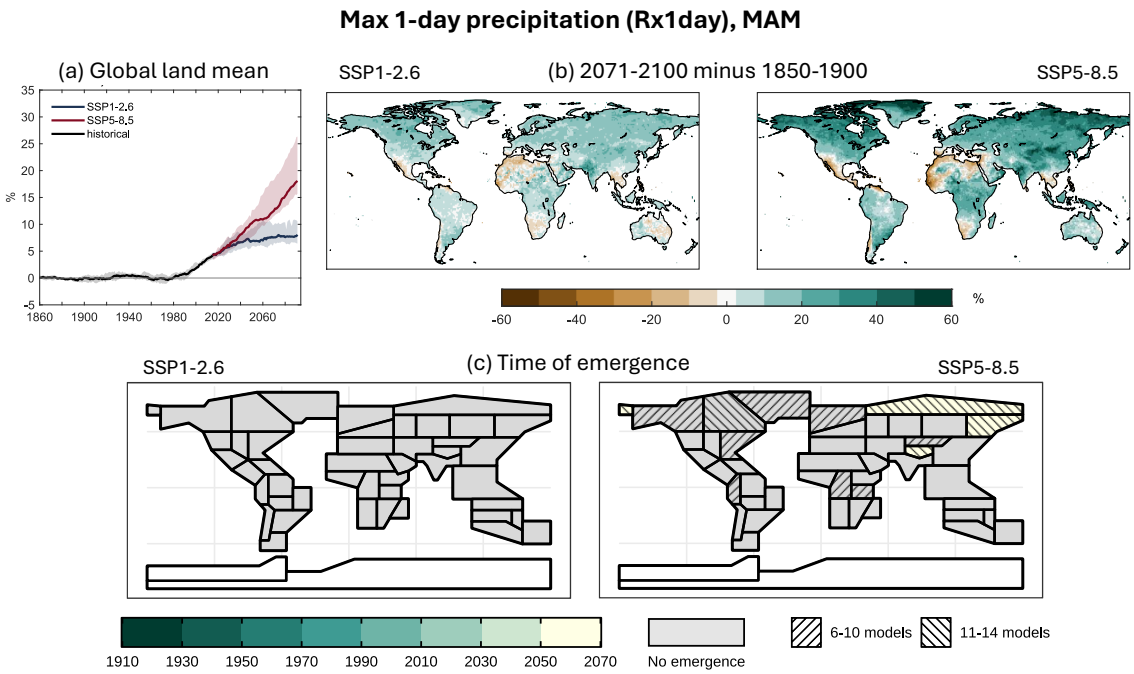

Figure S25. Same as Fig. S17, but for max 1-day precipitation (Rx1day) during March/April/May.

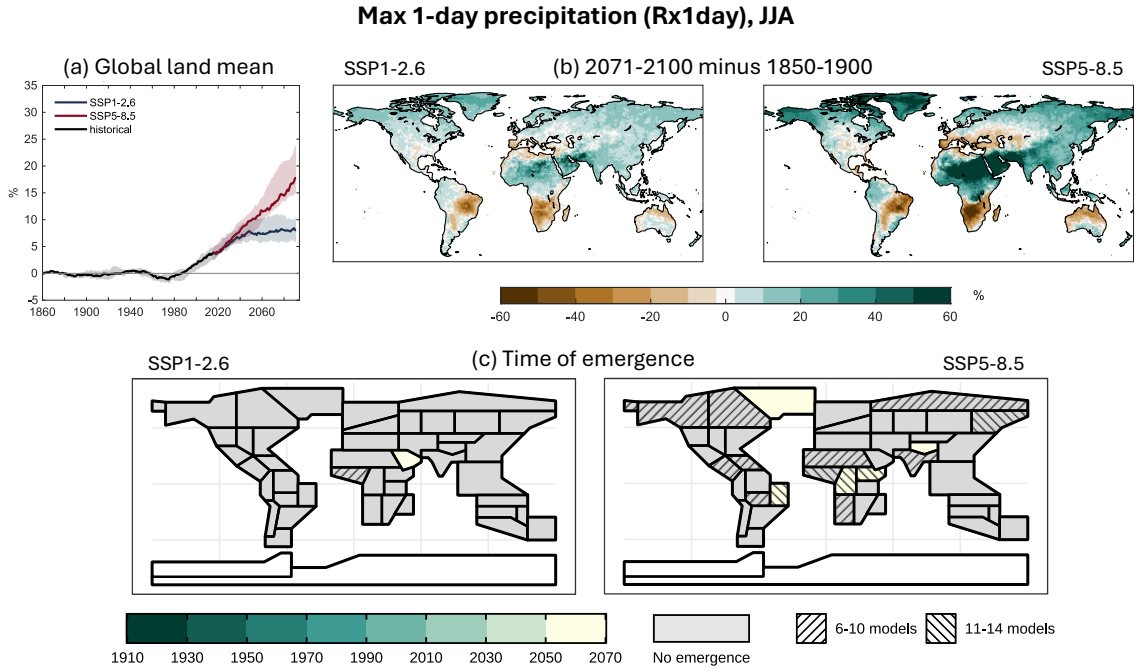

Figure S26. Same as Fig. S17, but for max 1-day precipitation (Rx1day) during June/July/August.

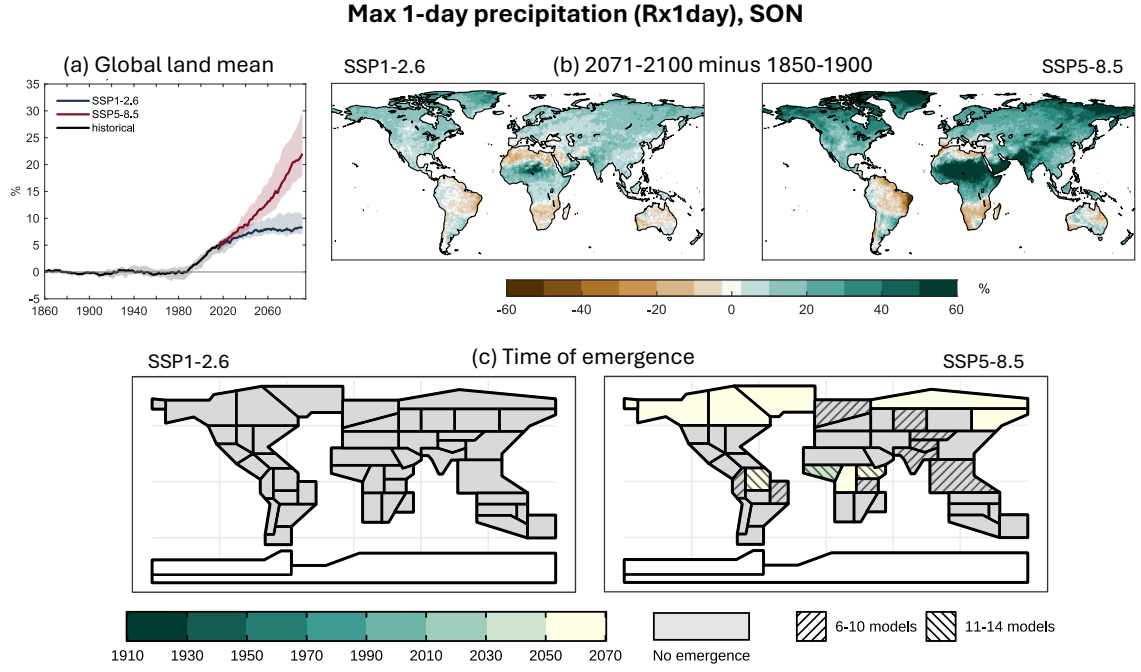

Figure S27. Same as Fig. S17, but for max 1-day precipitation (Rx1day) during September/October/November.